

Inducing intermittency in the inverse cascade of two dimensional turbulence by a fractal forcing

George Sofiadis and Ioannis E. Sarris

*Department of Mechanical Engineering, University of West Attica,
250 Thivon & P. Ralli Str., Egaleo, 122 44, Athens, Greece*

Alexandros Alexakis*

*Laboratoire de Physique de l'Ecole normale supérieure, ENS, Université PSL,
CNRS, Sorbonne Université, Université de Paris, F-75005 Paris, France*

(Dated: June 7, 2022)

We demonstrate that like in the forward cascade of three dimensional turbulence that displays intermittency (lack of self-similarity) due to the concentration of energy dissipation in a small set of fractal dimension less than three, the inverse cascade of two-dimensional turbulence can also display lack of self-similarity and intermittency if the energy injection is constrained in a fractal set of dimension less than two. A series of numerical simulations of two dimensional turbulence are examined, using different forcing functions of the same forcing length-scale but different fractal dimension D that varies from the classical $D = 2$ case to the point vortex case $D = 0$. It is shown that as the fractal dimension of the forcing is decreased from $D = 2$, the self-similarity is lost and intermittency appears, with the scaling of the different structure functions $\langle |\delta u_p|^p \rangle \propto r^{\zeta_p}$ differs from the dimensional analysis prediction $\zeta_p = p/3$. The present model thus provides a unique example that intermittency is controlled and can thus shed light and provide test beds for multi-fractal models of turbulence.

I. INTRODUCTION

Turbulence is pervasive in natural and industrial flows. In his first statistical description of turbulence Kolmogorov [1] argued that energy in turbulent flows cascades to smaller and smaller scales in such a way that there is a constant flux of energy from the large scales where energy is injected to the small viscous scales where energy is dissipated. Assuming further that this process is self-similar lead to the prediction that the different moments of velocity differences

$$S_p(r) \equiv \left\langle \left| \frac{\mathbf{r}}{r} \cdot (\mathbf{u}(\mathbf{x} + \mathbf{r}) - \mathbf{u}(\mathbf{x})) \right|^p \right\rangle \quad (1)$$

separated by a distance $r = |\mathbf{r}|$ scale like $S_p \propto r^{p/3}$ with the case $p = 3$ being an exact result (without the absolute value in eq.1). There is a mass of evidence however from the past years that this result is not exact; self-similarity is broken and the powers of velocity differences scale with different exponents $S_p(r) \propto r^{\zeta_p}$ where $\zeta_p \neq p/3$. This breaking of self-similarity is referred to as intermittency. It appears because as the cascade develops towards smaller scales, energy is concentrated in a set that occupies a smaller and smaller fraction of the domain volume so that finally energy dissipation is concentrated in a fractal set of dimension smaller than three [2, 3]. Modern theory of turbulence attempts to understand quantitatively the origin of intermittency and predict these exponents.

In two dimensions on the other hand, due to the presence of a second invariant, enstrophy, the energy cascades

in an inverse way from small to large scales [4]. This behavior was first predicted by Kraichnan–Leith–Batchelor (KLB) theory [5–7]. What was equally interesting was that the inverse cascade of energy in two dimensions is in fact self-similar so that all moments of velocity differences scale with r with exponents $\zeta_p = p/3$ [8]. This is explained by the fact that larger eddies extract energy from an ensemble of smaller eddies averaging out this way any extreme events. As energy moves up in scale it is not restricted in a set of dimension other than two. This behavior however does not always have to be the case as we argue in this work. If the energy injection in two dimensional turbulence is not space filling but is restricted in a set of dimension D smaller than two then as energy moves up in scale it can occupy larger and larger area fraction so that only at the largest scale it is concentrated in a two-dimensional set.

Fractal forcing is not just an abstract construction. In engineering it has been employed extensively in three dimensional turbulence with the use of fractal grids in simulations and experiments in order to enhance turbulence [9–13] but not as far as we know in two dimensions. In nature, atmospheric and oceanic flows are close to two-dimensional. When driven by winds over rough topography [14, 15] resemble two-dimensional turbulence driven by a fractal forcing. Furthermore, quasi-two-dimensional flows are believed to transition to an inverse cascade in a critical manner [3]. In such flows the energy injected in the two-dimensional manifold appears in a set of smaller dimension occupying a fraction of the domain area that approaches zero as criticality is approached [16, 17].

In this work we show using an extensive set of numerical simulations that indeed intermittency can appear in the inverse cascade of energy when the energy-injection

* alexakis@phys.ens.fr

N	512	1024	2048	4096
λ	16	32	64	128
Re_α	$2.2 \cdot 10^4$	$1.4 \cdot 10^5$	$8.9 \cdot 10^5$	$5.6 \cdot 10^6$

TABLE I. Resolution N , scale separation $\lambda = L/\ell_f$ and hypo-viscous Reynolds number Re_α .

mechanism is restricted to a set of fractal dimension $D < 2$. This model does not only give new insights in two-dimensional turbulence but also provides a unique example that intermittency is controlled and can thus provide test beds for multi-fractal models of turbulence.

II. NUMERICAL SIMULATIONS

We begin by considering the incompressible flow in a double periodic square domain of side $2\pi L$. In terms of the vorticity ω the two dimensional Navier-Stokes equation can be written as

$$\partial_t \omega + \mathbf{u} \cdot \nabla \omega = \nu \nabla^2 \omega + \alpha \nabla^{-2} \omega + f_\omega \quad (2)$$

where the velocity \mathbf{u} is linked to ω by $\omega = \nabla \times \mathbf{u}$, ν is the viscosity and α is a hypo-viscosity used to absorb energy arriving at the largest scales at a rate $\epsilon_\alpha = \langle |\nabla^{-1} \mathbf{u}|^2 \rangle$. The curl of the forcing is given by f_ω that injects energy at a rate ϵ at a lengthscale ℓ_f . Given f_ω there are three independent non-dimensional control numbers: the Reynolds number $Re = \epsilon^{1/3} \ell_f^{4/3} / \nu$, the hypo-viscous Reynolds number $Re_\alpha = \epsilon^{1/3} \ell_f^{-8/3} / \alpha$ and the domain to forcing scale ratio $\lambda = L/\ell_f$. This system of equations was solved numerically using the pseudo-spectral code GHOST [18] with $2/3$ de-aliasing and second order Runge-Kutta method for the time advancement. Since we are interested in the inverse cascade the Reynolds numbers was kept fixed to small value $Re = 10$. This value of Re is sufficiently large to allow for the development of the inverse cascade but suppresses the forward enstrophy cascade and any intermittency related to it. As a result the smallest scales in the system are given by ℓ_f and energy in these scales is concentrated close to the forcing. The hypo-viscous Reynolds number Re_α was set to $Re_\alpha = 10\lambda^{8/3}$ so that the large scale dissipation lengthscale ℓ_α remains fixed and close to the domain size $\ell_\alpha \simeq L$. Five different resolutions N were used varying λ as given in the table I.

Finally, five different forcing functions of different fractal dimension D are considered. The first one corresponding to $D = 2$ is the classical random forcing where all Fourier modes of wave-vectors \mathbf{k} satisfying $|\mathbf{k}| \simeq 1/\ell_f$ are forced with random phases. The $D = 1$ forcing corresponds to four vertical and four horizontal vortex lines with Gaussian profiles of width ℓ_f randomly placed in the domain. Similarly $D = 0$ corresponds to eight point-vortexes with Gaussian profile of width ℓ_f randomly placed in the domain. The $D = 3/2$ and $D = 1/2$

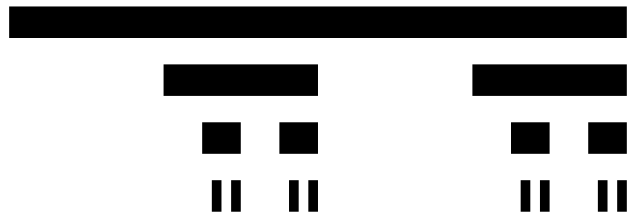


FIG. 1. Demonstration of how a fractal set of dimension $1/2$ is formed. At every step (down) the initial set is split in 4 equal sub-sets out of which subset 1 and 3 are disregarded.

correspond to Cantor sets that are constructed as follows. For $D = 3/2$ a dense set of horizontal and vertical vortex-lines are uniformly placed in the domain. This set is split in four equal subsets from which subset one and three are removed. The remaining sets are then split again in four from which again subset one and three are removed and so on, as demonstrated in figure 1, until no further splitting can be done. The resulting box-counting dimension is $D = 3/2$ [19]. For $D = 1/2$ we start with point-vortexes placed along one vertical and one horizontal line and we follow the same procedure leading this time to a box-counting dimension $D = 1/2$. For all forcing functions the forcing lengthscale ℓ_f was fixed so that the peak of the forcing spectrum was around similar wavenumber $k_f \simeq 1/\ell_f$. Furthermore, in all cases the amplitude of the forcing function was varied randomly delta-correlated in time fixing thus the energy injection rate ϵ . A color plot of the forcing functions for the five forcing functions is shown in the upper panels of figures 2. For this figure we used the smallest λ (largest ℓ_f) so that the point-vortexes in the left panel are clearly visible.

III. RESULTS

All forcing functions lead to an inverse cascade of energy marked by an energy spectrum close to $k^{-5/3}$ (top panel of figure 3) and a negative flux of energy $\Pi(k) = \langle \mathbf{u}_k^< \cdot (\mathbf{u} \cdot \nabla \mathbf{u}) \rangle$ (where $\mathbf{u}_k^<$ indicates the field \mathbf{u} filtered so that only wavenumbers with $|\mathbf{k}| \leq k$ are kept) shown in the lower panel of figure 3. The flux is approximately constant for the $D \geq 1$ cases but due to the relative small Re and the fact that the peak of the forcing spectrum for the cases $D = 3/2$ and $D = 2$ is slightly higher, the flux is affected by finite Re effects displaying a decrease close to the forcing scales.

Although all the five cases have an inverse cascade they do not have the same turbulent statistical behavior. This can already be seen in the vorticity plots shown in the lower panels of figure 2. Turbulence, marked by intense vorticity regions, is uniformly spread in the domain for the $D = 2$ case but as D is decreased intense vorticity regions occupy a smaller area fraction but with larger intensity. In order to quantify this observation we plot in figure 4 the probability distribution function (p.d.f.)

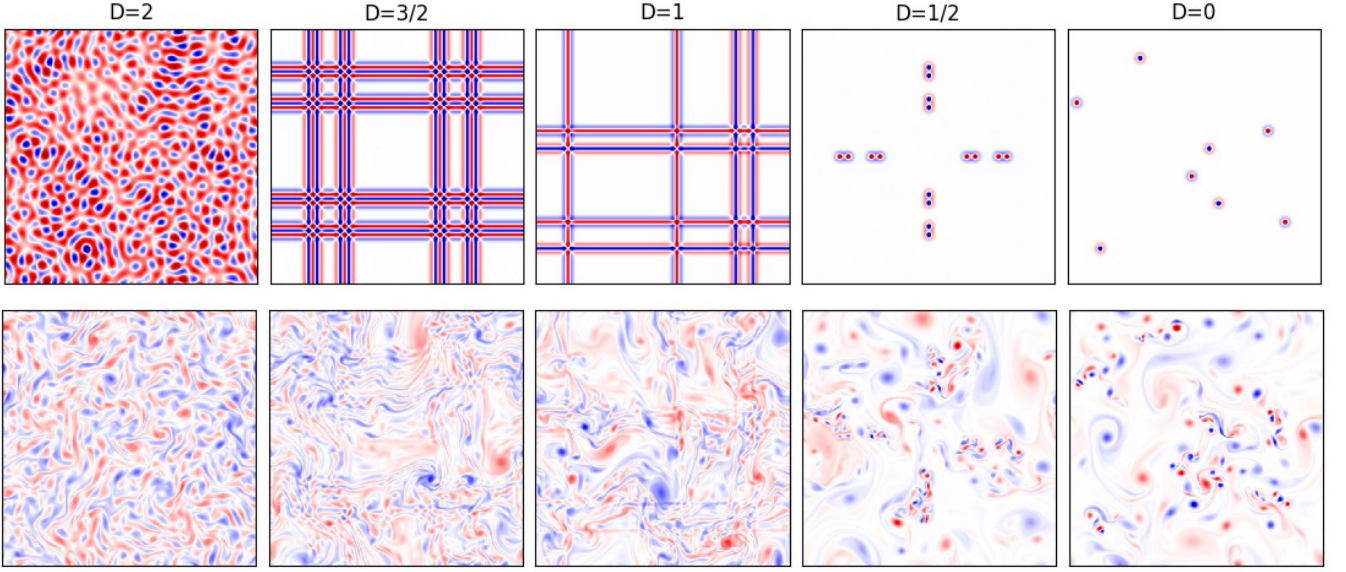


FIG. 2. Top panels: Random forcing function for different dimension D at resolution $N = 512$. Lower panels: Vorticity of the flow for the same cases as above at steady state.

of velocity differences for the two extreme cases $D = 2$ and $D = 0$ for different values of r starting from the largest $r = L/4$ to the forcing scale $r = L/128 = \ell_f$. In the $D = 2$ case the p.d.f.s are close to Gaussian for all examined r . Furthermore, no significant change is observed as r is varied: ie they are self-similar. In the $D = 0$

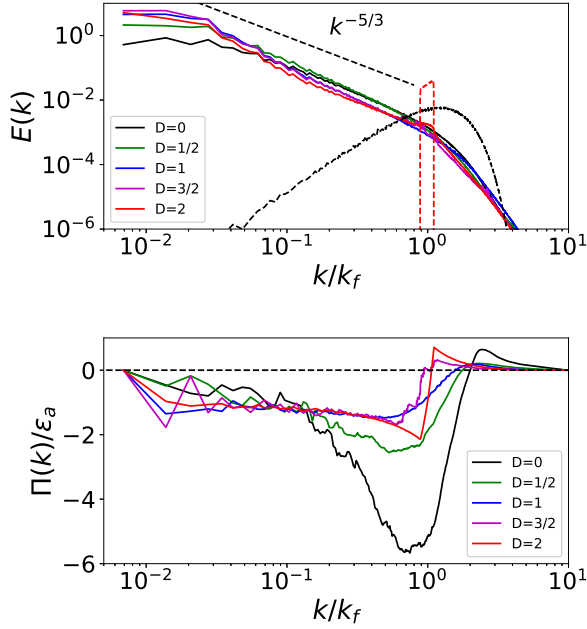


FIG. 3. Top: Energy spectra for the highest resolution runs. The dashed lines give the forcing spectrum for the two extreme cases $D = 2$ and $D = 0$. The straight dashed line gives the $k^{-5/3}$ scaling. Bottom: Energy flux for the same cases.

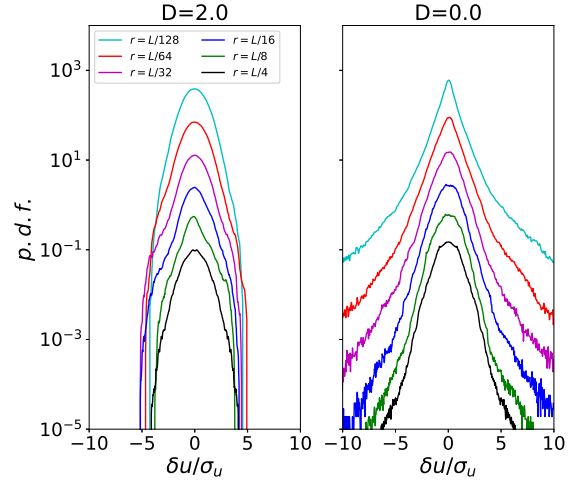


FIG. 4. The probability distribution function of $\delta u(r)$ normalized by its variance $\sigma_u = S_2(r)^{1/2}$ for different values of r and for $D = 2$ left and $D = 0$ right. The curves have been shifted vertically for clarity.

case on the other hand the p.d.f.s deviate from the Gaussian distribution having large tails. Most importantly, as smaller values of r are considered the deviations from Gaussianity become stronger with the distribution becoming more peaked and with stronger tails. In other words self-similarity is lost for the $D = 0$ case.

A quantitative way to measure this lack of self-similarity, is to measure the kurtosis $K(r) = S_4(r)/S_2^2(r)$. Kurtosis gives a measure of how heavy-tailed is the distribution of δu . $K(r) = 3$ corresponds to a Gaussian dis-

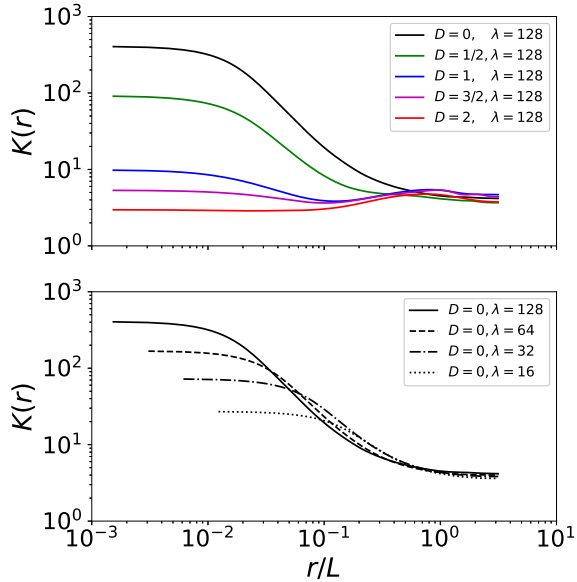


FIG. 5. The top panel shows $K(r)$ for the flows at highest λ for the five different forcing functions. The lower panel shows $K(r)$ for $D = 0$ and four different values of λ .

tributed field while larger values correspond to fields of wider distribution. If the distribution is self-similar $K(r)$ will be independent of r . In figure 5 we plot the Kurtosis for different cases. The top panel shows $K(r)$ for the flows at highest $\lambda = 128$ (highest resolution) for the five different forcing functions. For $D = 2$, $K(r)$ is almost flat and close to 3, indicating that δu follows a self-similar, nearly-Gaussian distribution. As the dimension of the forcing is decreased $K(r)$ takes larger and larger values in the small r range, with the $D = 0$ case having two orders of magnitude larger $K(\ell_f)$ than a Gaussian field. The lower panel shows the case $D = 0$ for the different values of λ . As λ and Re_α are increased the non-self-similar behavior extends to a larger range of r with the deviation from Gaussianity increasing. Therefore this amounts to a phenomenon that persists and extends as the infinite Re_α and infinite box-size limit is reached.

The result of figure 5 already indicates that ζ_2 and ζ_4 can not follow the scaling $\zeta_p = p/3$ that would imply an r independent Kurtosis. In figure 6 we plot the exponents ζ_p for all cases. The exponents were measured using the extended self-similarity assumption [20] to extend the range that a power-law behavior is observed where $S_p(r)$ is plotted as a function of $S_3(r)$ and assuming the theoretically predicted linear scaling of the third moment $S_3(r) \propto r$. The exponents up to $p = 6$ were calculated except for the $D = 0$ case that showed a particular slow convergence for the high p moments. For $D = 2$ the exponents follow the linear scaling $\zeta_p = p/3$. As D is decreased, the exponents with $p < 3$ increase while exponents with $p > 3$ decrease. The flow thus becomes more

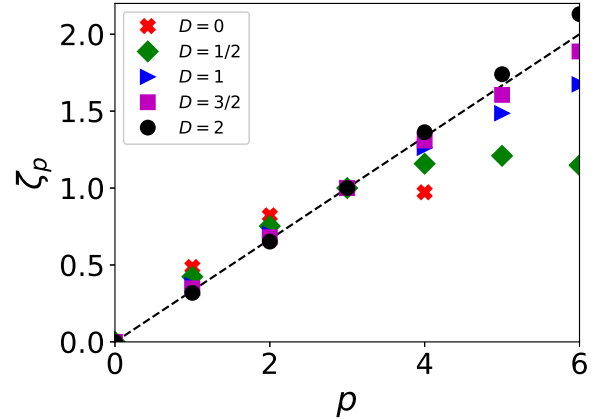


FIG. 6. Scaling exponents ζ_p for the five different D considered calculated using extended-self-similarity.

intermittent as D is decreased with the high order moments being dominated by few but strong events in the tail of the distribution.

IV. CONCLUSIONS

In this work we have shown, that the inverse cascade of energy can display intermittent features provided that the forcing function injects energy in fractal a set of dimension smaller than two. Intermittency is demonstrated by long tails in the distribution of the velocity differences at small scales caused by the forcing, that as larger scales are approached they flatten out becoming closer to Gaussian. This behavior was shown to persist as larger domains (larger λ) are considered and become stronger as the dimension D is decreased.

Here we employed only mono-fractal forcing. Bi-fractal, or multi-fractal forcing can also be considered by adding with appropriate weight different fractal forcing functions. This could lead to an intermittent behavior that is closer to the three dimensional cascade, (albeit in the opposite direction). More generalized fractal forcing functions that dynamically evolve could also be considered. Such functions could be examined in future work.

Most importantly the strength of intermittency caused by the fractal forcing is determined by its dimension and thus it provides a way to create a cascade for which the intermittency can be varied from self-similar to strongly intermittent. Ideas, about the behavior and origin of intermittency can thus be put in the test using this simple model. Finally one can ask how a fractal forcing can affect intermittency properties in three dimensional turbulence.

ACKNOWLEDGMENTS

This work was granted access to the HPC resources of MesoPSL financed by the Région Île-de-France and the project EquipMeso (project no. ANR-10-EQPX-29-01), of the HPC resources of GENCI-TGCC & GENCI-IDRIS

(project no. A0110506421) and the HPC facility ARIS from the Greek Research and Technology Network (GR-NET). AA is supported by the project Dysturb (project no. ANR-17-CE30-0004) financed by the Agence Nationale pour la Recherche (ANR).

-
- [1] A. N. Kolmogorov, The local structure of turbulence in incompressible viscous fluid for very large reynolds numbers, *Cr Acad. Sci. URSS* **30**, 301 (1941).
 - [2] U. Frisch, *Turbulence: the legacy of AN Kolmogorov* (Cambridge university press, 1995).
 - [3] A. Alexakis and L. Biferale, Cascades and transitions in turbulent flows, *Physics Reports* **767**, 1 (2018).
 - [4] G. Boffetta and R. E. Ecke, Two-dimensional turbulence, *Annual review of fluid mechanics* **44**, 427 (2012).
 - [5] G. K. Batchelor, Computation of the energy spectrum in homogeneous two-dimensional turbulence, *The Physics of Fluids* **12**, II (1969).
 - [6] R. H. Kraichnan, Inertial ranges in two-dimensional turbulence, *The Physics of Fluids* **10**, 1417 (1967).
 - [7] C. E. Leith, Diffusion approximation for two-dimensional turbulence, *The Physics of Fluids* **11**, 671 (1968).
 - [8] G. Boffetta, A. Celani, and M. Vergassola, Inverse energy cascade in two-dimensional turbulence: Deviations from gaussian behavior, *Physical Review E* **61**, R29 (2000).
 - [9] D. Hurst and J. Vassilicos, Scalings and decay of fractal-generated turbulence, *Physics of Fluids* **19**, 035103 (2007).
 - [10] K. Nagata, Y. Sakai, T. Inaba, H. Suzuki, O. Terashima, and H. Suzuki, Turbulence structure and turbulence kinetic energy transport in multiscale/fractal-generated turbulence, *Physics of Fluids* **25**, 065102 (2013).
 - [11] R. Seoud and J. Vassilicos, Dissipation and decay of fractal-generated turbulence, *Physics of fluids* **19**, 105108 (2007).
 - [12] S. Laizet and J. C. Vassilicos, Dns of fractal-generated turbulence, *Flow, turbulence and combustion* **87**, 673 (2011).
 - [13] B. Mazzi and J. C. Vassilicos, Fractal-generated turbulence, *Journal of Fluid Mechanics* **502**, 65 (2004).
 - [14] F. P. Bretherton and D. B. Haidvogel, Two-dimensional turbulence above topography, *Journal of Fluid Mechanics* **78**, 129 (1976).
 - [15] G. K. Vallis and M. E. Maltrud, Generation of mean flows and jets on a beta plane and over topography, *Journal of physical oceanography* **23**, 1346 (1993).
 - [16] S. J. Benavides and A. Alexakis, Critical transitions in thin layer turbulence, *Journal of Fluid Mechanics* **822**, 364 (2017).
 - [17] K. Seshasayanan, S. J. Benavides, and A. Alexakis, On the edge of an inverse cascade, *Physical Review E* **90**, 051003 (2014).
 - [18] P. D. Mininni, D. Rosenberg, R. Reddy, and A. Pouquet, A hybrid mpi-openmp scheme for scalable parallel pseudospectral computations for fluid turbulence, *Parallel computing* **37**, 316 (2011).
 - [19] H. Triebel, *Fractals and spectra: related to Fourier analysis and function spaces* (Springer Science & Business Media, 2010).
 - [20] R. Benzi, S. Ciliberto, R. Tripiccone, C. Baudet, F. Massaioli, and S. Succi, Extended self-similarity in turbulent flows, *Physical review E* **48**, R29 (1993).